Invited Articles

Diffusive mass transfer from a Janus sphere

Hassan Masoud 1,* and Jonathan P. Rothstein 2

¹Department of Mechanical Engineering-Engineering Mechanics, Michigan Technological University, Houghton, Michigan 49931, USA

²Department of Mechanical and Industrial Engineering, University of Massachusetts, Amherst, Massachusetts 01003, USA



(Received 21 January 2022; accepted 5 May 2022; published 6 July 2022)

We study the mixed boundary-value problem of finding the concentration distribution surrounding a two-sided (Janus) sphere, with a uniform concentration imposed on one segment of it and the no-mass-flux condition enforced on the other one. This mass transfer problem arises in the analysis of the Marangoni propulsion phenomenon, where a chemically active particle propels itself along a liquid-gas interface via nonuniform release of a chemical species that locally alters the surface tension distribution. Assuming that the mass transfer is purely driven by diffusion (i.e., neglecting advection), we present an approximate form for the concentration field derived from the integral representation of the solution to the corresponding Laplace equation. We demonstrate the high fidelity of the proposed approach by comparing its results with those obtained from a collocation method based on the series solution of the problem. Beyond the motivating problem, our findings are expected to be applicable to the self-diffusiophoresis of catalytic colloids, as well as to the conduction heat transfer and electrostatics problems involving partially insulated spheres. Moreover, our approach can lead to the derivation of similarly accurate approximate solutions to analogous problems in mathematical physics.

DOI: 10.1103/PhysRevFluids.7.070501

I. INTRODUCTION

Mixed boundary-value problems commonly arise in potential theory [1], with applications in the areas of heat and mass transfer, flow of inviscid fluids, electrostatics, elasticity, etc. We recently came across a problem of this kind when studying the Marangoni-driven motion of a chemically active spherical surfer along a water-air interface [2]. In that context, a chemical species (such as alcohol, whose concentration is linearly related to the surface tension at the interface) is discharged from the active side of the surfer, while no exchange of mass occurs on the surfer's remaining surface. This asymmetric release upsets the balance of surface tension acting on the surfer and also generates a Marangoni flow around it, which together result in the propulsion of the surfer. When the advective transport of mass is negligible (i.e., the limit of zero Peclet number), the problem of determining the concentration distribution of the released active agent can be formulated as a mixed boundary-value problem governed by the Laplace equation. Once this problem is solved, the propulsion speed of the surfer can be calculated analytically in the limit of zero Reynolds number, where the effect of inertia is weak (see, e.g., Refs. [3–6]).

Here, we present an approximate, yet very accurate, solution for the problem of finding a harmonic function (denoting the concentration field of the released chemical species) that decays to zero at infinity, and satisfies a uniform distribution on one segment and zero-normal-gradient

^{*}hmasoud@mtu.edu

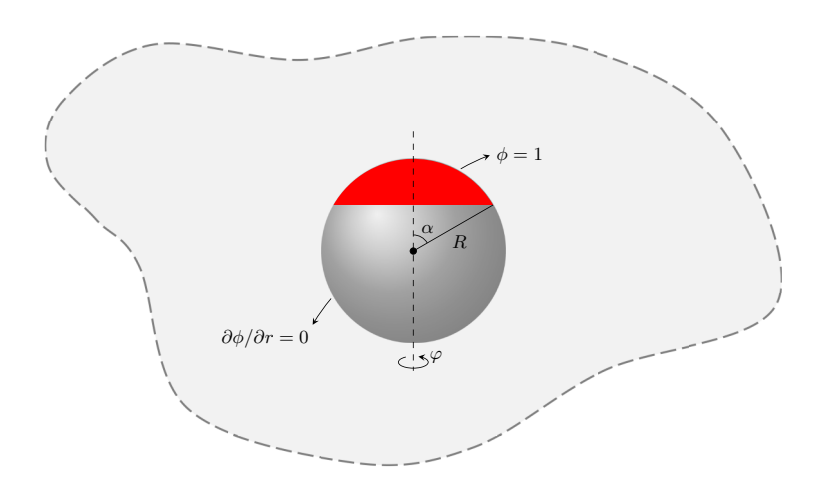


FIG. 1. Mass release from a Janus sphere into an unbounded domain. The sphere has active and inert sides that are modeled by uniform concentration and no-flux boundary conditions, respectively.

condition on the remainder of a spherical surface. To the best of our knowledge, an exact analytical solution for this problem is not currently available in the literature. Our derivation is based on an integral representation of the solution, which reduces the original problem to solving a Fredholm integral equation of the second kind for the distribution of the scalar function on the impermeable surface of the sphere. We discuss the advantage of this approach over a perhaps more conventional method, which uses the separation of variables and eigenfunction expansion to construct the solution.

II. PROBLEM STATEMENT AND SOLUTION

Consider the Laplace equation

$$\nabla^2 \phi = 0 \tag{1}$$

outside a sphere of radius R (see Fig. 1), with the boundary conditions

$$\phi = 1$$
 at $r = 1$ for $0 \le \theta \le \alpha$, $\frac{\partial \phi}{\partial r} = 0$ at $r = 1$ for $\alpha < \theta \le \pi$, and $\phi \to 0$ as $r \to \infty$. (2)

Here, $\phi = (c - c_\infty)/(c_s - c_\infty)$ and c denote, respectively, the normalized and dimensional concentration fields, with c_s and c_∞ being the values of c at the active surface of the sphere (see Fig. 1) and far away from it, respectively. Additionally, α is a constant angle and (r, θ, φ) are the components of a dimensionless spherical coordinate system, in which r = 1 represents the surface of the sphere. As will be clear shortly, it is useful to extend the domain of ϕ to also include the region inside the sphere, where ϕ still satisfies the Laplace equation while maintaining a continuous value at r = 1, i.e.,

$$\lim_{r \to 1^{-}} \phi = \lim_{r \to 1^{+}} \phi. \tag{3}$$

Conventionally, the extended ϕ can be expanded in series of spherical harmonics as

$$\phi = \begin{cases} \sum_{n=0}^{\infty} C_n \frac{P_n(\cos \theta)}{r^{n+1}} & \text{for } r \geqslant 1\\ \sum_{n=0}^{\infty} C_n r^n P_n(\cos \theta) & \text{for } r < 1 \end{cases}$$
(4)

where

$$\sum_{n=0}^{\infty} C_n P_n(\cos \theta) = 1 \quad \text{for} \quad 0 \leqslant \theta \leqslant \alpha \quad \text{and} \quad \sum_{n=0}^{\infty} C_n(n+1) P_n(\cos \theta) = 0 \quad \text{for} \quad \alpha < \theta \leqslant \pi,$$
(5)

with $\{C_n\}$ and P_n being constant coefficients and the Legendre polynomial of degree n, respectively. It can be shown [from Eqs. (4) and (5)] that the radial derivative of ϕ is discontinuous at the surface of the sphere. Denoted by Γ , this jump in the normal gradient can be calculated via

$$\Gamma = \lim_{r \to 1^{-}} \frac{\partial \phi}{\partial r} - \lim_{r \to 1^{+}} \frac{\partial \phi}{\partial r} = 2j - \phi_{s}, \tag{6}$$

where the subscript s indicates evaluation at r=1 and $j=-\lim_{r\to 1+}\partial\phi/\partial r$. As noted previously in the literature (see, e.g., Ref. [7]) and also discussed in Sec. III, the above series solution suffers from very slow convergence and oscillatory behavior despite its relatively simple form. Hence, here we develop an alternative solution strategy that is not prone to the same drawbacks. The details of our approach are as follows.

Let the extended ϕ be

$$\phi = \phi_1 + \phi_2,\tag{7}$$

where

$$abla^2 \phi_1 = 0$$
, with $\phi_1 = 1$ at $r = 1$ for $0 \le \theta \le \alpha$,
 $\Gamma_1 = 0$ at $r = 1$ for $\alpha < \theta \le \pi$, and $\phi_1 \to 0$ as $r \to \infty$, (8)

and

$$abla^2 \phi_2 = 0$$
, with $\phi_2 = 0$ at $r = 1$ for $0 \le \theta \le \alpha$,
 $\Gamma_2 = \Gamma$ at $r = 1$ for $\alpha < \theta \le \pi$, and $\phi_2 \to 0$ as $r \to \infty$. (9)

The field ϕ_1 corresponds to the concentration distribution surrounding a zero-thickness shell of spherical-cap shape (see the red area in Fig. 1) that is maintained at unit concentration on both sides (see, e.g., Sec. 1.1 and Sec. 8.7.1 of Ref. [1]). This field can be expressed in closed form as (see Ref. [7])

$$\phi_1 = \frac{2}{\pi} \left(\frac{1+r}{2r} \sin^{-1} A_1 - \frac{|r-1|}{2r} \sin^{-1} A_2 \right),\tag{10}$$

where

$$A_1 = \frac{(1+r)\sqrt{1-\cos\alpha}}{\sqrt{B+(1+r)^2 - 2r(\cos\alpha + \cos\theta)}}, \quad A_2 = \frac{|r-1|\sqrt{1-\cos\alpha}}{\sqrt{B+(r-1)^2 + 2r(\cos\alpha - \cos\theta)}}, \quad \text{and}$$

$$B = \sqrt{(r^2 - 1)^2 - 4r(\cos\alpha - r\cos\theta)(\cos\theta - r\cos\alpha)}.$$
 (11)

Following Ref. [7], ϕ_2 also may be written formally as

$$\phi_2 = \frac{4}{\pi} \sqrt{\frac{4+\eta^2}{r}} \int_{\kappa}^{\eta/\mu} \frac{1}{\sqrt{\eta^2 - \mu^2 \hat{\eta}^2}} \int_{\lambda}^{\infty} \frac{\hat{\hat{\eta}}}{\sqrt{\hat{\hat{\eta}}^2 - \lambda^2}} \frac{\Gamma}{(4+\hat{\hat{\eta}}^2)^{3/2}} \, d\hat{\hat{\eta}} \, d\hat{\eta}, \tag{12}$$

where

$$\eta = 2\tan(\theta/2), \quad \hat{\eta} = 2\tan(\hat{\theta}/2), \quad \hat{\hat{\eta}} = 2\tan(\hat{\theta}/2), \quad \lambda^2 = \hat{\eta}^2 \left| \frac{\eta^2 + 4(\mu^2 - 1) - \hat{\eta}^2}{\eta^2 - \mu^2 \hat{\eta}^2} \right|,$$

$$\mu^2 = 1 + \frac{(r - 1)^2 (4 + \eta^2)}{16r}, \quad \kappa = \frac{1}{2} \left[\sqrt{(\eta + \nu)^2 + \chi} - \sqrt{(\eta - \nu)^2 + \chi} \right], \quad \nu = 2\tan(\alpha/2), \quad \text{and}$$

$$\chi = \frac{(r - 1)^2 (4 + \eta^2)(4 + \nu^2)}{16r}.$$
(13)

It is worth noting that Γ represents the density of mass sources/sinks distributed on the surface of the sphere, and its value, along the interval $[\alpha, \pi]$, is equal to [see Eq. (6)]

$$\Gamma = -\phi_s = -(\phi_{1.s} + \phi_{2.s}),\tag{14}$$

where [from Eqs. (10) and (11)]

$$\phi_{1,s} = \frac{2}{\pi} \sin^{-1} \left[\frac{\sin(\alpha/2)}{\sin(\theta/2)} \right] \quad \text{for} \quad \theta \in [\alpha, \pi].$$
 (15)

Rewriting Eq. (12) in terms of θ [with the help of the definitions given in Eq. (13)] and evaluating it at r = 1, we then arrive at

$$\Gamma = -\left(\phi_{1,s} + \frac{1}{2\pi} \int_{\alpha}^{\theta} \frac{1}{\sqrt{\cos\hat{\theta} - \cos\theta}} \int_{\hat{\theta}}^{\pi} \frac{\Gamma \sin\hat{\hat{\theta}}}{\sqrt{\cos\hat{\theta} - \cos\hat{\hat{\theta}}}} d\hat{\hat{\theta}} d\hat{\theta}\right) \quad \text{for} \quad \theta \in [\alpha, \pi]. \quad (16)$$

With the derivation of Eq. (16), we have reduced the original problem to that of solving a Fredholm integral equation of the second kind for the distribution of Γ (or $\phi_{2,s}$, since $\phi_{1,s}$ is known) on the impermeable segment of the sphere. Absent a closed-form solution, a standard approach for tackling this problem is to construct an iterative solution in the form of

$$\Gamma_{n+1} = -\left(\phi_{1,s} + \frac{1}{2\pi} \int_{\alpha}^{\theta} \frac{1}{\sqrt{\cos\hat{\theta} - \cos\theta}} \int_{\hat{\theta}}^{\pi} \frac{\Gamma_n \sin\hat{\hat{\theta}}}{\sqrt{\cos\hat{\theta} - \cos\hat{\hat{\theta}}}} d\hat{\hat{\theta}} d\hat{\theta}\right),$$
where $n = 0, 1, \dots$ and $\Gamma_0 = -\phi_{1,s}$. (17)

However, achieving reasonable accuracy via this technique requires several iterations, which involve calculating deeply nested integrals. To avoid this issue, we opt to directly approximate Γ . To this end, we take our cue from Eq. (17). In particular, we first note that, to the leading order, Γ can be approximated as $\Gamma_0 = -\phi_{1,s}$. Then, upon inspecting the difference between Γ_0 and Γ_1 , we deduce that this rough estimate can be refined by considering

$$\Gamma \approx -(\phi_{1s})^{\tau},\tag{18}$$

provided that $\tau \geqslant 1$. We choose to determine the value of the exponent τ systematically by fixing the average error of the proposed approximation over the surface of the sphere to zero, i.e.,

$$\int_0^\pi e \sin\theta \ d\theta = 0,\tag{19}$$

where

$$e = (\phi_{1,s})^{\tau} - \phi_{1,s} + \frac{1}{2\pi} \int_{\alpha}^{\theta} \frac{1}{\sqrt{\cos \hat{\theta} - \cos \theta}} \int_{\hat{\theta}}^{\pi} \frac{(\phi_{1,s})^{\tau} \sin \hat{\hat{\theta}}}{\sqrt{\cos \hat{\theta} - \cos \hat{\theta}}} d\hat{\theta} d\hat{\theta}. \tag{20}$$

Enforcing Eq. (19) ensures that no net mass flux emanates from the inactive side of the sphere.

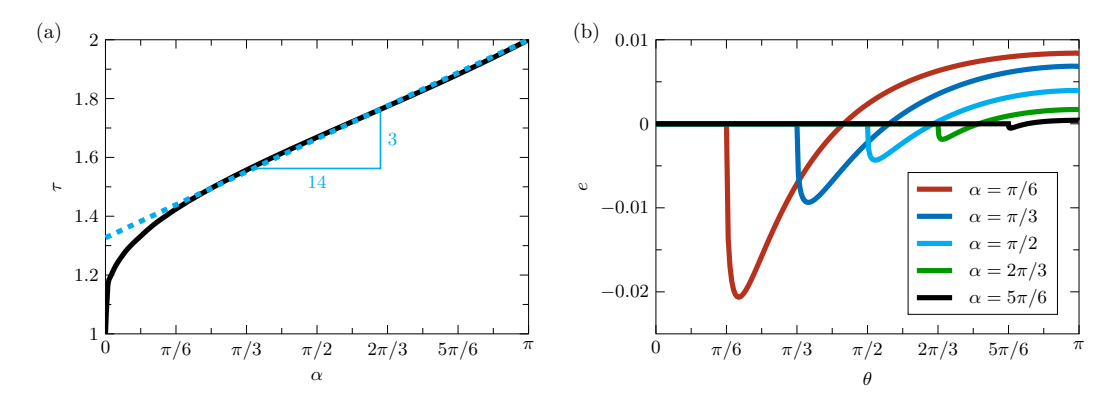


FIG. 2. (a) The plot of τ versus α overlaid by a dashed line of slope 3/14 passing through the point $(\pi, 2)$. (b) The plots of approximation error, as defined by Eq. (20), versus θ for $\alpha = \pi/6, \pi/3, \pi/2, 2\pi/3, 5\pi/6$.

Figure 2(a) displays the variation of τ as a function of α . We see that, when α is very small, τ sharply rises from one with increasing α from zero. The rise of τ continues, although with a decreasing slope, as α further increases, and, for α greater than $\pi/6$, τ follows a linear growth path until it reaches the value of 2 at $\alpha = \pi$. As demonstrated by the dashed line in Fig. 2(a), the variations of τ in this latter region are very well captured by the line

$$\tau = 2 + \frac{3}{14}(\alpha - \pi). \tag{21}$$

With τ known, we assess the accuracy of our approximation through the evaluation of e for representative values of α [see Fig. 2(b)]. As it can be seen, the error stays very low in all cases (especially for $\alpha \geqslant \pi/2$), confirming the fidelity of the proposed semiempirical approach. It is important to point out that using Eq. (21), instead of Eq. (19), for calculating τ does not substantially change the behavior of the error plots presented in Fig. 2(b). Hence, one could employ the explicit relation for τ expressed in Eq. (21) in the range $[\pi/6, \pi]$, with no significant loss of accuracy.

III. RESULTS AND DISCUSSION

Encouraged by the outcome of the self-check presented in Fig. 2(b), in this section, we discuss how several quantities of interest vary with changing α . Specifically, we consider the distributions of ϕ_s and j on, respectively, the impermeable ($\alpha < \theta \leqslant \pi$) and active ($0 \leqslant \theta \leqslant \alpha$) segments of the Janus sphere (see Fig. 3), which are calculated from

$$\phi_s = \phi_{1,s} - \frac{1}{2\pi} \int_{\alpha}^{\theta} \frac{1}{\sqrt{\cos \hat{\theta} - \cos \theta}} \int_{\hat{\theta}}^{\pi} \frac{(\phi_{1,s})^{\tau} \sin \hat{\hat{\theta}}}{\sqrt{\cos \hat{\theta} - \cos \hat{\theta}}} d\hat{\theta} d\hat{\theta}$$
 (22)

and

$$j = \frac{\phi_s + \Gamma}{2} = \frac{1 + \Gamma}{2},\tag{23}$$

where we have (see Ref. [7])

$$\Gamma = \frac{2}{\pi} \left(\sqrt{\frac{1 + \cos \alpha}{\cos \theta - \cos \alpha}} + \tan^{-1} \sqrt{\frac{\cos \theta - \cos \alpha}{1 + \cos \alpha}} \right) + \frac{1}{\pi \sqrt{\cos \theta - \cos \alpha}} \int_{\alpha}^{\pi} \frac{\sqrt{\cos \alpha - \cos \hat{\theta}} \left(\phi_{1,s}\right)^{\tau} \sin \hat{\theta}}{\cos \theta - \cos \hat{\theta}} d\hat{\theta}.$$
(24)

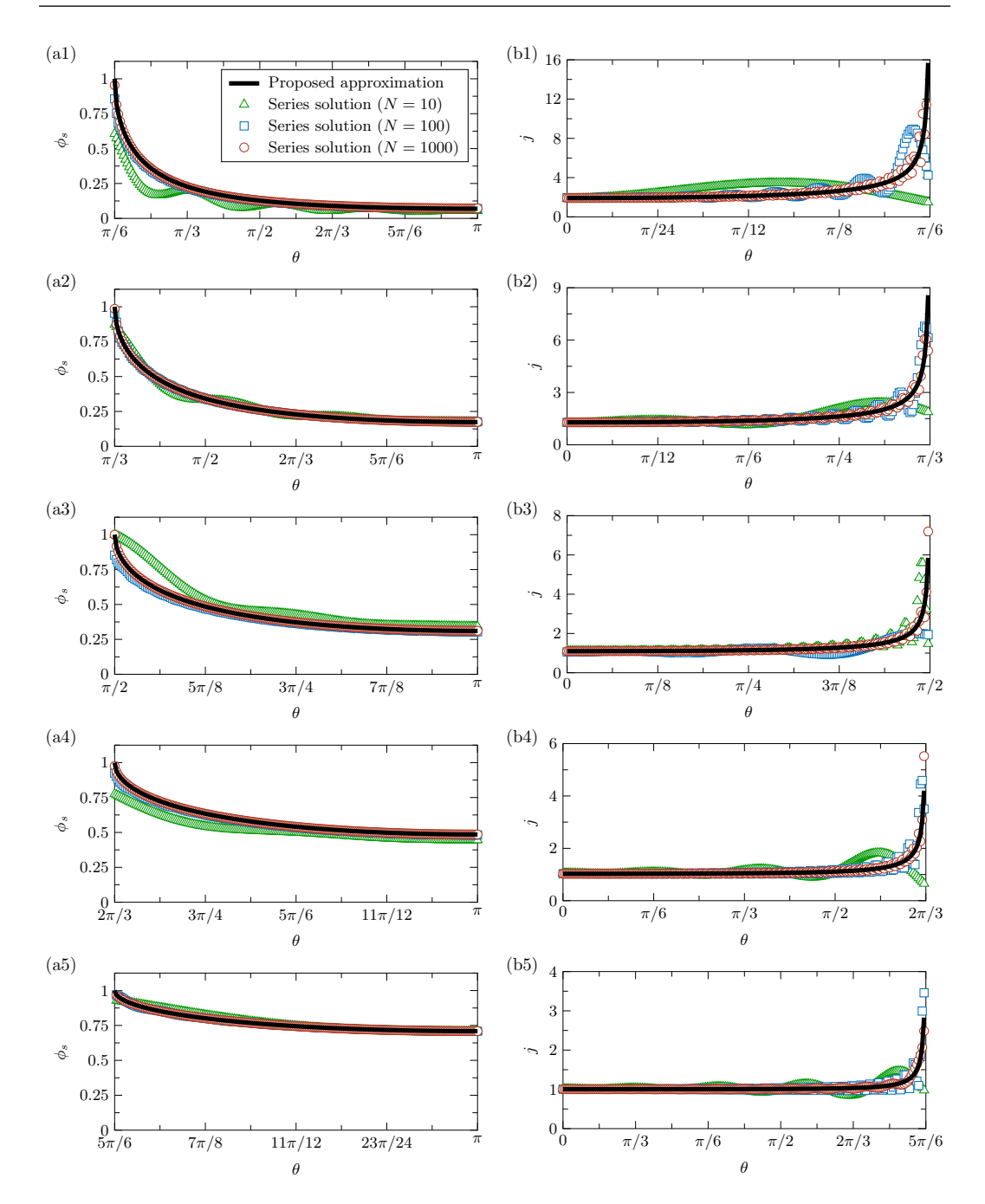


FIG. 3. The plots of the dimensionless (a) concentration distribution ϕ_s and (b) local mass flux j versus θ on, respectively, the impermeable and active segments of the Janus sphere. The subfigure numbers 1, 2, ..., 5 correspond to $\alpha = \pi/6, \pi/3, \pi/2, 2\pi/3, 5\pi/6$, respectively.

We also consider the variations of

$$J = 2\pi \int_0^{\pi} j \sin \theta \ d\theta = 2\pi \int_0^{\pi} \phi_s \sin \theta \ d\theta = 2\pi \left[1 - \cos \alpha + \int_{\alpha}^{\pi} (\phi_{1,s})^{\tau} \sin \theta \ d\theta \right]$$
 (25)

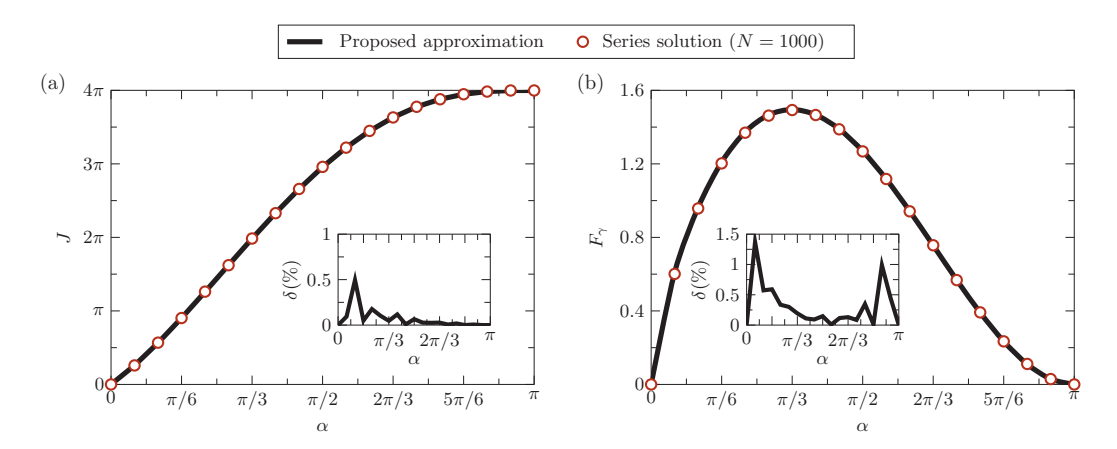


FIG. 4. The plots of the dimensionless (a) total mass flux J [see Eq. (25)] and (b) representative of the net surface tension force F_{γ} [see Eq. (26)] versus α . The insets show the percentage difference (denoted by δ) between the results of our approximation and those obtained from the series solution described by Eq. (4), with N = 1000.

and

$$F_{\gamma} = 2 \int_{0}^{\pi} \phi_{s} \cos \theta \ d\theta = 2 \left(\sin \alpha + \int_{\alpha}^{\pi} \phi_{s} \cos \theta \ d\theta \right)$$
 (26)

as functions of α (see Fig. 4). Here, the first quantity is the total mass flux from the sphere and the second one is a representative of the net surface tension force acting on the sphere in the context of Marangoni propulsion (see, e.g., Refs. [2–4] and the first paragraph of Sec. I). Note that the second equality in Eq. (25) is derived from Green's second identity (see, e.g., Refs. [8,9]).

To further highlight the accuracy of our approximate formulation for the concentration field, we plot its results, in Figs. 3 and 4, along with the results obtained from Eq. (4), where the series solution is truncated to N terms and the coefficients C_n are determined by solving a linear system of algebraic equations arising from the enforcement of Eq. (5) at N+1 evenly distributed points on the surface of the sphere in the direction of the polar angle θ . As a side note, due to the orthogonality of Legendre polynomials, $J = 4\pi C_0$.

There are several observations that can be made from the plots of Fig. 3. First, we see that the curves of ϕ_s versus θ are very steep in the neighborhood of α when this angle is small (see the graphs in the left column). Yet, as α increases, the curves tend to flatten out and, eventually, (although not shown) they turn into horizontal lines for $\alpha = \pi$. Second, for j, we see a singular and also discontinuous behavior at $\theta = \alpha$, except for when $\alpha = \pi$ (see the graphs in the right column). Specifically, j blows up as $1/\sqrt{\alpha-\theta}$ when θ approaches α [see Eqs. (23) and (24)]. Away from the singularity, however, the curves are well behaved and, similar to those for ϕ_s , become flatter with increasing α . In addition to these observations, we also learn from Fig. 3 that the series solution expressed in Eq. (4) converges quite slowly. This is particularly obvious from the mass flux plots, where, even with 1001 terms included (i.e., N=1000), getting oscillation-free results in a consistent manner is still out of reach. That it takes a large number of terms to construct an accurate representation of the concentration field is a major pitfall of the collocation-based solution described by Eq. (4).

Next, concerning the integrated quantities J and F_{γ} , we see that the former follows a nearly linear relation with α (with an approximate slop of 6) for $\alpha \lesssim \pi/2$, and that (as expected) it approaches 4π when α nears π [see Fig. 4(a)]. On the other hand, Fig. 4(b) shows that F_{γ} initially increases with α , reaches a maximum at $\alpha \approx \pi/3$, and then declines back to zero with further increasing of α to π . Furthermore, consistent with the results of Fig. 3, the plots of Fig. 4 (including the insets)

indicate that the predictions of our approximate solution closely match the results obtained from the series solution when a sufficiently large number of terms are considered. As one might anticipate, better matches are seen for integrated quantities than for local ones.

IV. SUMMARY

We examined a mixed boundary-value mass transfer problem that was motivated by the study of Marangoni propulsion. We proposed and verified a semiempirical method of solution and analyzed its results. In addition to providing the sought-after insights into the motivating problem, our findings may also be applicable to the self-diffusiophoresis of chemically active particles (see, e.g., Refs. [10,11]), and some problems in conduction heat transfer and electrostatics involving partially insulated spheres. More generally, we hope that our approach inspires future approximate solutions to similar problems that arise in mathematical physics.

ACKNOWLEDGMENTS

Financial support from the National Science Foundation under Grants No. CBET-1749634 (H.M.) and No. CBET-1705519 (J.P.R.) is acknowledged. We also thank S. J. Kang and E. Dehdashti for stimulating discussions.

- [1] I. N. Sneddon, *Mixed Boundary Value Problems in Potential Theory* (North-Holland Publishing Company, Amsterdam, 1966)
- [2] S. Jafari Kang, S. Sur, J. P. Rothstein, and H. Masoud, Forward, reverse, and no motion of Marangoni surfers under confinement, Phys. Rev. Fluids 5, 084004 (2020).
- [3] H. Masoud and H. A. Stone, A reciprocal theorem for marangoni propulsion, J. Fluid Mech. 741, R4 (2014).
- [4] V. Vandadi, S. J. Kang, and H. Masoud, Reverse marangoni surfing, J. Fluid Mech. 811, 612 (2017).
- [5] D. Crowdy, Collective viscous propulsion of a two-dimensional flotilla of marangoni boats, Phys. Rev. Fluids 5, 124004 (2020).
- [6] D. Crowdy, Viscous propulsion of a two-dimensional marangoni boat driven by reaction and diffusion of insoluble surfactant, Phys. Rev. Fluids 6, 064003 (2021).
- [7] V. I. Fabrikant, Closed form solution to some mixed boundary value problems for a charged sphere, J. Aust. Math. Soc. Ser. B **28**, 296 (1987).
- [8] H. Masoud and H. A. Stone, The reciprocal theorem in fluid dynamics and transport phenomena, J. Fluid Mech. 879, P1 (2019).
- [9] V. Vandadi, S. Jafari Kang, and H. Masoud, Reciprocal theorem for convective heat and mass transfer from a particle in Stokes and potential flows, Phys. Rev. Fluids 1, 022001(R) (2016).
- [10] R. Golestanian, T. B. Liverpool, and A. Ajdari, Designing phoretic micro-and nano-swimmers, New J. Phys. 9, 126 (2007).
- [11] M. N. Popescu, W. E. Uspal, and S. Dietrich, Self-diffusiophoresis of chemically active colloids, Eur. Phys. J. Spec. Top. 225, 2189 (2016).